LBL--33345

DE93 007711

Presented at the XXII International Symposium on Multiparticle Dynamics,
Santiago de Compostela, Spain, July 13-17, 1992.
Proceedings will be published by the World Scientific Company.

Results from the NA36 on Strangeness Production in 200 GeV/c per nucleon S + Pb and p + Pb reactions

Douglas E. Greiner
Lawrence Berkeley Laboratory
University of California, Berkeley, CA 94720

and

The NA36 Collaboration

July 1992

This work was supported by the Director, Office of Energy Research, Division of Nuclear Physics of the Office of High Energy and Nuclear Physics of the U.S. Department of Energy under Contract DE-AC03-76SF00098

Results from NA36 on Strangeness Production in 200 GeV/c per nucleon S + Pb and p + Pb reactions.

Douglas E. Greiner representing the NA36 Collaboration

E. Andersen[1] , P.D. Barnes[8], R. Blaes[10], M. Cherney[7], B. de la Cruz[6], G.E. Diebold[8], B. Dulny[5], C. Fernández[9], G. Franklin[8], C. Garabatos[9], J.A. Garzón[9], W. Geist[10], D.E. Greiner[2], C.R. Gruhn[2,a], M. Hafidouni[10], J. Hrubec[11], P.G. Jones[3,b], E.G. Judd[3], J.P.M. Kuipers[12,a], M. Ladrem[10], P. Ladrón de Guevara[6], G. Løvhøiden[1], J. MacNaughton[11], J. Mosquera[9], Z. Natkaniec[5], J.M. Nelson[3], G. Neuhofer[11], W.C. Ogle[2], C.Perez de los Heros[6], M. Pló[9], P. Porth[11], B. Powell[4], B. Quinn[8], A. Ramil[9], H. Rohringer[11], I. Sakrejda[2,d], T.F. Thorsteinsen[1], J. Traxler[11], C. Voltolini[10], K. Wozniak[5], A. Yañez[9], Y. Yee[2] and R. Zybert[3].

NA 36 mailing address: NA 36, c/o Dr. D. E. Greiner, Mailstop 50D, Lawrence Berkeley Laboratory 1 Cyclotron Road, Berkeley CA 94720, USA

1) University of Bergen, Dept. of Physics, N-5007 Bergen, Norway
2) Lawrence Berkeley Laboratory (LBL), Berkeley CA 94720, USA
3) University of Birmingham, Dept. of Physics, Birmingham B15 2TT, UK
4) European Organization for Nuclear Research (CERN), CH-1211 Genève 23, Switzerland
5) Instytut Fizyki Jadrowej, PL-30 055 Krakow 30, Poland
6) CIEMAT, Div. de Física de Partículas, E-28040 Madrid, Spain
7) Creighton University, Department of Physics, Omaha, Nebraska 68178, USA
8) Carnegie-Mellon University, Dept. of Physics, Pittsburgh PA 15213, USA
9) Universidad de Santiago, Dpto. Física de Partículas, E-15706 Santiago de Compostela, Spain
10) Centre de Recherches Nucléaires , IN2P3-CNRS/Université L. Pasteur, BP 20, F 67037 Strasbourg, France
11) Institut für Hochenergiephysik (HEPHY), A-1050 Wien, Austria
12) University of York, Dept. of Physics, York Y01 5DD, UK

a) Present address: CERN, PPE division
b) Present address: Lawrence Berkeley Laboratory, Berkeley CA 94720, USA

Abstract

Recent results from CERN experiment NA36 are discussed and compared with models. These results refer to reactions of sulfur and protons of momentum 200 GeV/c per nucleon on a lead target. The Λ spectrum for the sulfur beam was found to peak at mid-rapidity rather than target rapidity as observed in the proton induced reactions. This result indicates different reaction mechanisms are active. We discuss in some detail the analysis methods used. The data are consistent with the assumption of a fireball of high strangeness content being created at mid-rapidity in S + Pb reactions.

1. Introduction

The NA36 experiment was proposed to examine strangeness production in ion-ion collisions. One of the most robust signals of quark-gluon plasma production is the excessive emission of strange particles from the reaction.[1] The yields of neutral strange particles Λ , $\bar{\Lambda}$ and K^0 were detected by observation of their charged decay modes using a

Time Projection Chamber (TPC). The data reported here were taken in 1990 with 200 GeV/c per nucleon sulfur and proton beams on a lead target.[2] This report includes some details of the methods used for signal extraction and correction.

2. Apparatus, Data and Resolution.

The NA36 experimental apparatus is shown schematically in Fig. 1.

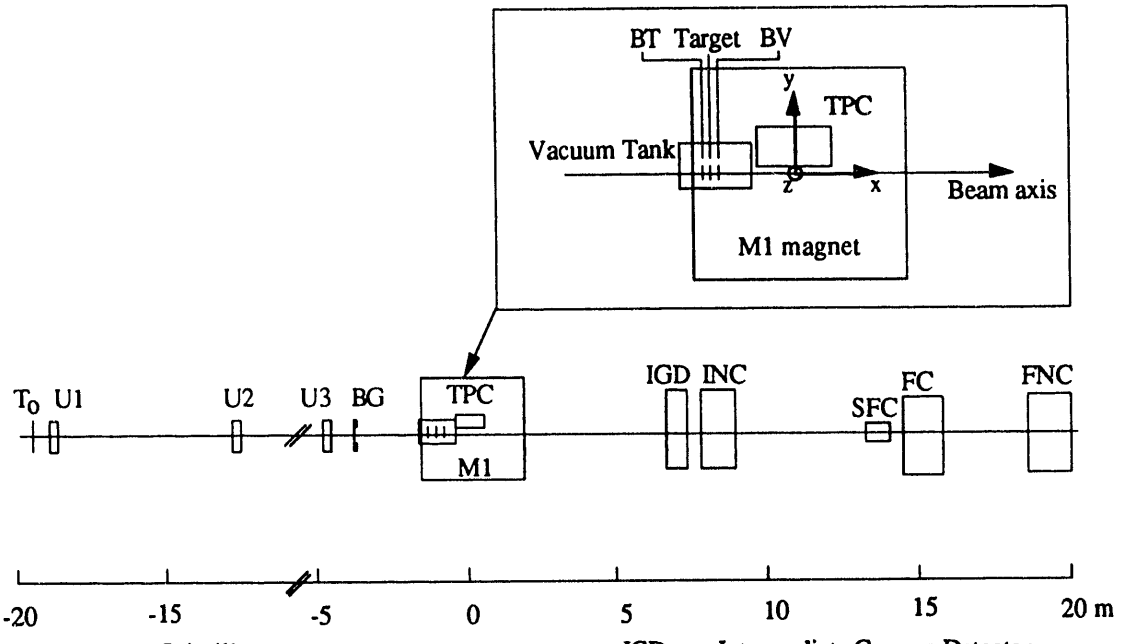

T_0	Scintillator	IGD	Intermediate Gamma Detector
U1, U2, U3	Multiwire Proportional Chambers	INC	Intermediate Neutral Calorimeter
BG	Beam Geometry Counters	SFC	Small Forward Čerenkov
BT, BV	Silicon Detectors	FC	Forward Čerenkov
TPC	Time Projection Chamber	FNC	Forward Neutral Calorimeter

Fig. 1. NA36 experimental setup.

The chambers U1, U2 and U3 were used to measure the incoming beam trajectory thus providing the position of each event at the target. The TPC recorded the trajectories of charged particles in the 3 Tesla field of the M1 magnet. This allowed the determination of the momentum of all tracks as well as the sign of their charge. The TPC (Fig. 2) was specially designed to enhance the two track resolution. The signals were detected by short anode wires (1 cm) spaced 2.54 mm apart. This is unlike the usual cathode pad readout where two track resolution is limited because the image charge distribution of adjacent tracks become superimposed. The advantage of anode readout is that the avalanche is seen directly on the closest anode wire. This method provided about 5 mm two-track resolution and also allowed significant cost and data reductions as it was only necessary to read out the time of the pulses and not their amplitude. The spatial resolutions achieved were 1.05 mm in the bend plane and 1.77 mm in the drift direction, which met with the design specifications.

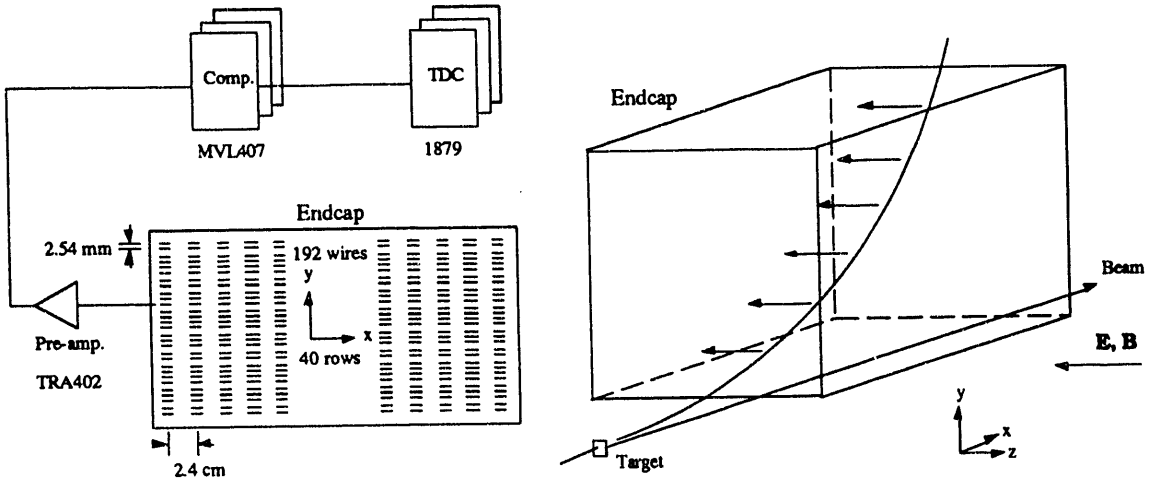

Fig. 2 NA36 TPC and readout electronics.

The anode readout design provided efficient detection of tracks in the very high particle density region closest to the target. Shown in Fig. 3 are the track densities observed in the central collisions of S + Pb. The pickup region is in the back of the TPC where the track finding software begins the process of track reconstruction. The tracks are well defined before they are followed into the maximum density region in the front of the TPC. The single track detection efficiency including all instrumental and analysis effects degrades only slightly with event multiplicity remaining above, 70% even at the highest multiplicities as shown in Fig. 4.

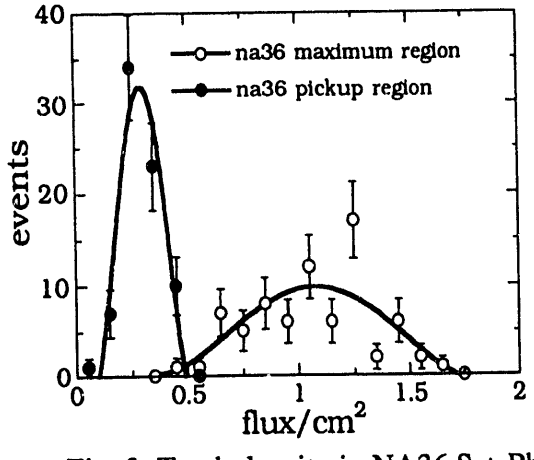

Fig. 3 Track density in NA36 S + Pb data

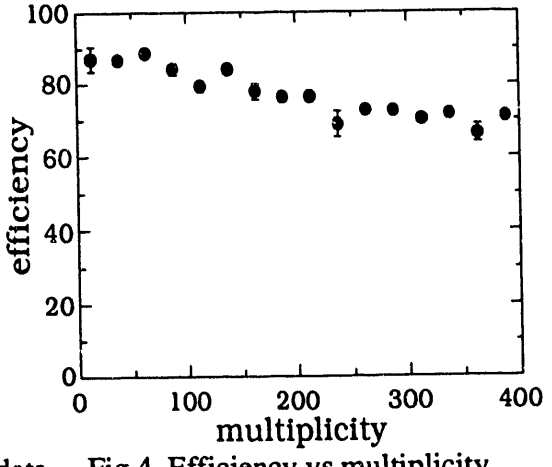

Fig.4 Efficiency vs multiplicity.

3. Data Sample and Signal Extraction.

This report is based on a data sample of 2.2 million events taken with a trigger mix of 45% central (b<6 fm), 45% minimum bias and 10% beam. The admixture of triggers allowed trigger normalization and the extraction of absolute production cross sections. Simple geometric cuts were first applied to filter the reconstructed V^0 candidates and significantly reduce the combinatorial background. The total detected yields were Λ – 30000, $\bar{\Lambda}$ - 10000 and K^o - 24000.

The Podolanski-Armenteros plot for the final sample is shown in Fig. 5. The high statistics and low background result in a strong and clear signal for Λ, $\bar{\Lambda}$ and K^o. The small opening angle for the electron pairs coming from the γ conversion places them at the bottom of the plot and makes them easy to eliminate.

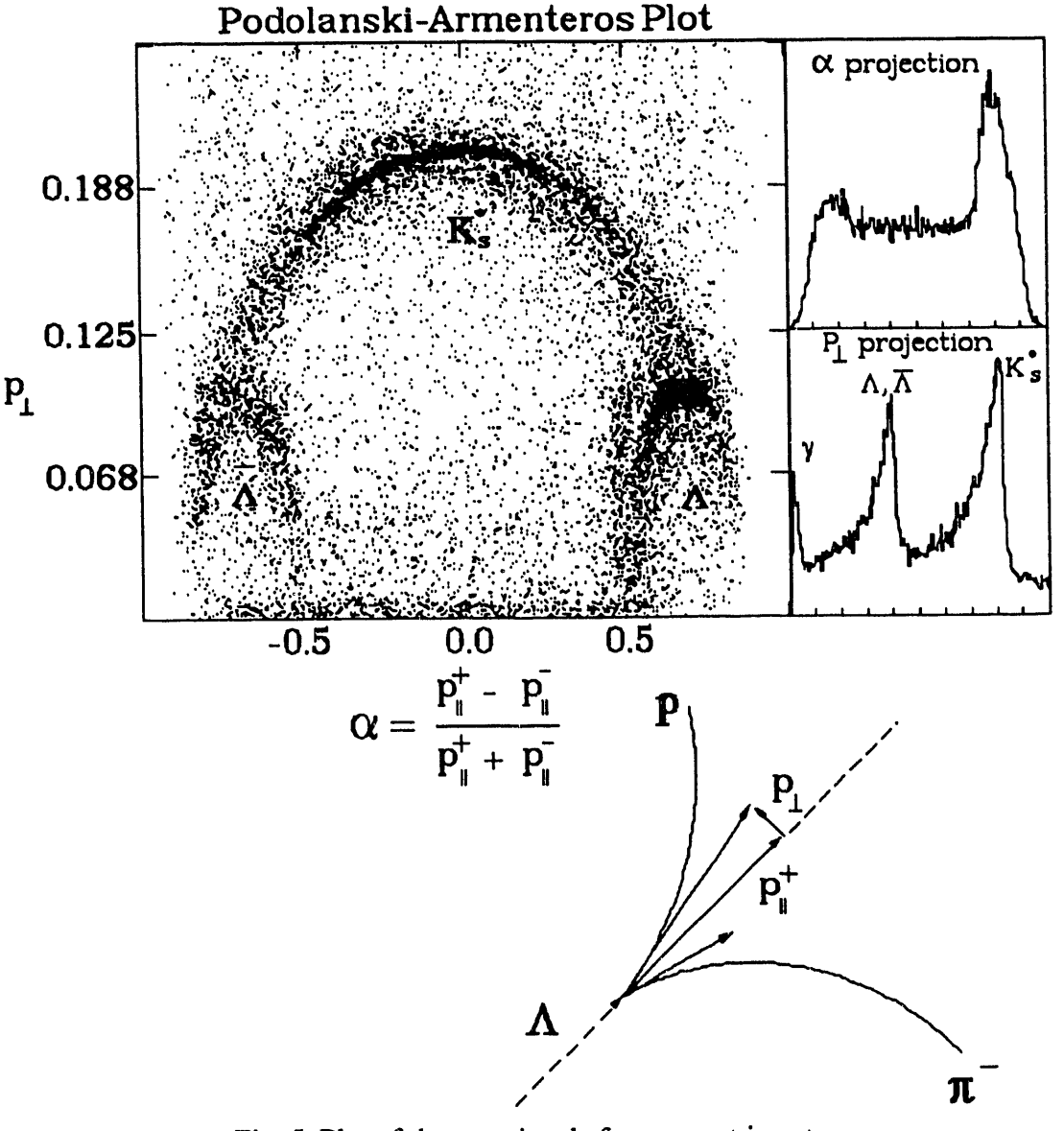

Fig. 5 Plot of the raw signal after geometric cuts.

The mass resolutions integrated over the data sample were 6 Mev for Λ, $\bar{\Lambda}$ and 8 MeV for K^0 respectively. The high statistics data also facilitated background removal. To evaluate the signal for a specific bin of rapidity, transverse momentum or event multiplicity, a trigger weighted mass histogram of the raw data in that bin was made. Fig. 6 shows the mass plot for the Λ signal in the region $2.00 < y < 2.25$, this plot is summed over all P_t and multiplicity. The signal is clearly seen over a smooth background. The background was studied with Monte Carlo techniques and found to consist of a combinatorial component and a component due to the kinematic regions where the signals are almost identical for Λ and K^0, or $\bar{\Lambda}$ and K^0. These regions can be seen on the Podolanski-Armenteros plot near $\alpha \cong \pm 0.75$. Signal extraction was achieved by fitting signal+background to the mass distributions. These curves are also shown individually in Fig. 6.

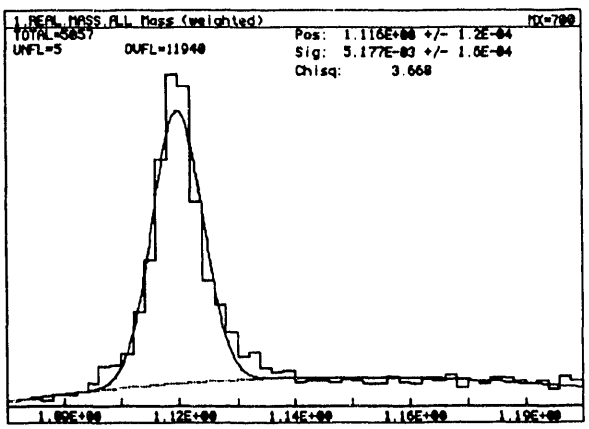

Fig. 6 Raw mass histogram.

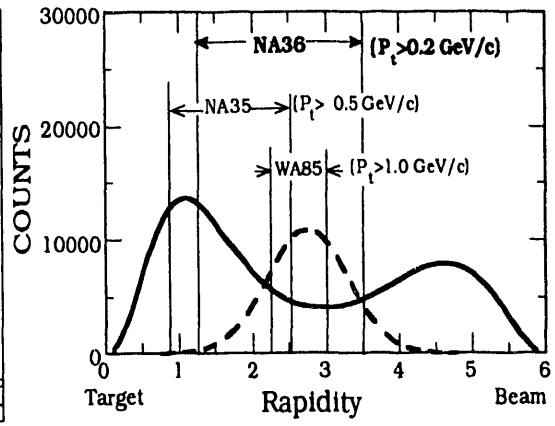

Fig.7 Acceptance comparison.

The acceptance of NA36 was identified as the region where we had sufficient statistics to apply the background subtraction method described above. This acceptance region is shown in Fig. 7, where comparison is also made with the experiments NA35 and WA85. Also shown in Fig. 7 are the expected rapidity distributions of Λ (solid curve) and $\bar{\Lambda}$ (dashed curve) from the Fritiof 1.7 generator. The larger coverage of NA36 allows studies to be made of signal dependence on rapidity and transverse momentum.

4. Strangeness Enhancement

The question is whether ion - ion collisions produce more strange particles than one would expect from p + p or p + A results. The NA35 experiment found that the Λ production per negative track was enhanced for S + S collisions and that the enhancement actually increases with multiplicity.[3] Experiment WA85 found that for central collisions of S + Pb there was a general enhancement but that the enhancement did not increase with rapidity density.[4] The disagreement could possibly be due to the fact that WA85 triggers on only very central events. Since the NA36 trigger covers a wide range of event multiplicities we have been able to resolve this question.

In order to examine the number of strange particles per negative track we need to extract a measure of the event negative multiplicity from our data. To do this we have used a the technical Monte Carlo for the NA36 configuration. Our approach to the simulation of NA36 data was to use the emperical TPC response to tune the simulation to accurately reproduce the observed response. Measurements of resolution and efficiency were performed on representative tracks and then compared with simulated tracks of the same

momentum. The simulation program was adjusted till the results were identical. One of the crucial parameters is the TPC efficiency and its dependence on particle momentum. The comparison of efficiency seen for data and the Monte Carlo versions of the same tracks is shown in Fig. 8. The distributions of relevant track properties such as pull distributions etc were compared in all momentum intervals. A particularly sensitive comparison is the χ^2 probability. The comparison for tracks between 2 and 3 GeV/c per nucleon momentum is shown in Fig. 9.

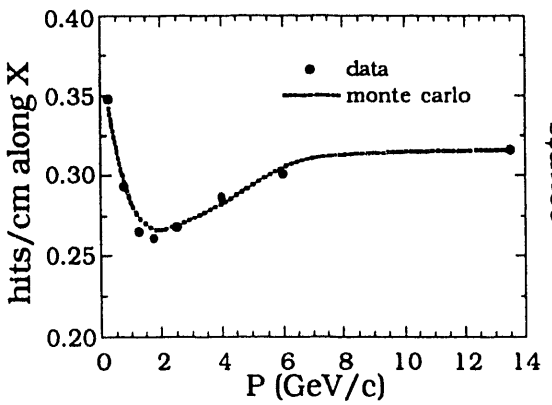

Fig. 8 TPC efficiency vs momentum

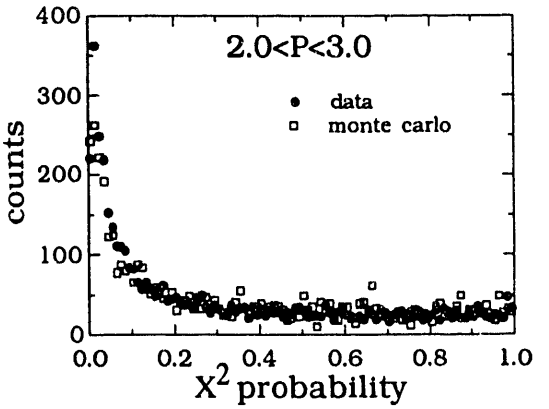

Fig. 9 Fit probability data and Monte.Carlo

Having established the ability of the Monte Carlo to reproduce the properties of individual tracks we now turn to complete events. Exactly how tracks merge and how the analysis software recognizes them determines the observed number of tracks in the TPC. The only input to the Monte Carlo relative to these effects is the simulation of the overlap of signal pulses on the individual anode wires. In order to test the accuracy of the observed tracks in the TPC for minimum bias events we compared data and events generated by the technical Monte Carlo. We chose Fritiof 1.7 as the event generator because it has been shown to reproduce the multiplicity distributions in collisions of this type.[5] This is a stringent test of the entire Monte Carlo program because the number of tracks seen in the TPC is not simply dependent on the target used but on all the secondary production of particles in all the various gases and other materials in the experimental apparatus. The comparison between the multiplicity of NA36 minimum bias and Monte Carlo data shown in Fig.10 is strong evidence that the simulation accurately describes the experimental response.

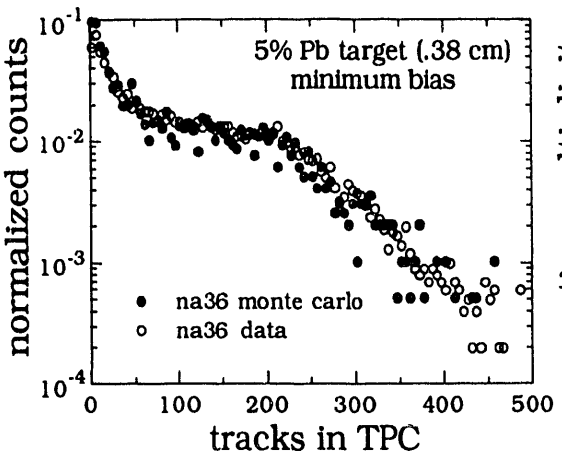

Fig. 10 Multiplicity of data and simulation

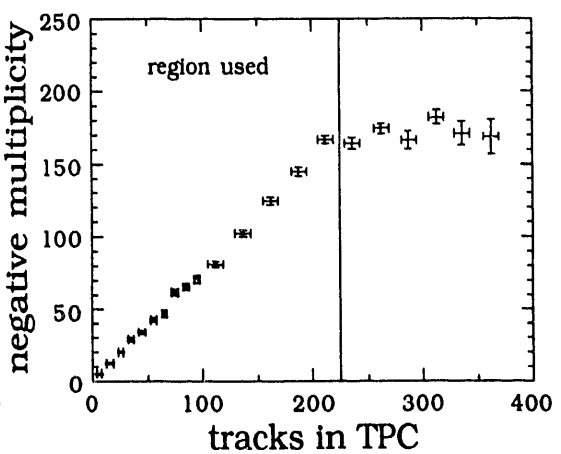

Fig.11. Determination of negative multiplicity.

Having verified that the simulation of the number of tracks in the TPC agrees well with the data it is natural, therefore, to examine the relationship between tracks in the TPC and the actual negative multiplicity in the input Monte Carlo events. This is shown in Fig.11. As one would expect there is a well behaved correlation between negative multiplicity of the event and number tracks observed in the TPC. The deviation from a linear behavior at high multiplicities is due to spiraling tracks which are seen by the analysis software as multiple tracks. The observed correlation is used to assign a negative multiplicity to each data event in our studies of strangeness enhancement.

The enhancement of strangeness is measured by comparison of S + Pb with p + Pb data taken with the same apparatus. The comparison of yield per negative track is shown in Fig.12a,b,c in all cases we see that the yield of strange particles per negative track is about twice that observed in p + Pb reactions. There is a clear dependence on event multiplicity for the Λ and K^o produced in S + Pb reactions. The yield rises at low multiplicities and saturates in the region of a negative multiplicity of 50. This resolves the discrepancy between NA35 and WA85 results because the NA35 data were taken in the relatively low multiplicity environment of minimum bias S + S collisions while the WA85 data were taken in S + W collisions at the highest multiplicities. The origin of this multiplicity dependence is not understood. The effect is larger than possible kinematic acceptance effects as evidenced by the Fritiof 7.0 curves (The Fritiof 7.0 result for K^o is known to be an overprediction. It over predicts p + p data) and may be an indication that when the number of participants of the reaction increases beyond a certain value new reaction mechanisms come into play. Possibilities range from various re-interaction scenarios to quark-gluon plasma production.

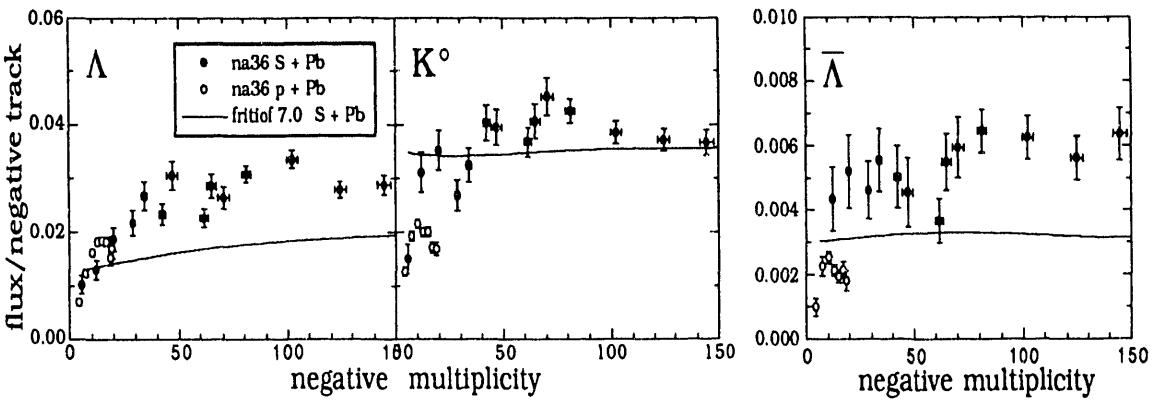

Fig. 12a,b,c Flux of Λ, K^o and $\bar{\Lambda}$ per negative track.

5. Transverse Momentum

In Fig. 13 we show the transverse momenta of Λ, $\bar{\Lambda}$ and K^o in S + Pb reactions. These spectra are dominated by events in the mid-multiplicity range (about 100-200 tracks in the TPC). The slope of the transverse momentum spectra are usually related to a "temperature" of the reactions. This concept is strictly applicable only to a perfectly equlibrated system. Our data are integrated over all impact parameters and it is not probable that such an assumption is fulfilled. However, it has been found that the transverse momentum spectra are well fit by the formulation and it provides a measure of violence and a means of comparing different sets of data. We measure temperatures rather close to 200 MeV for the three particle choices. This is a value that is much higher than that seen in p + p reactions and is consistent with the critical temperatures predicted using lattice gauge calculations for the phase transition to quark-gluon plasma.[6]

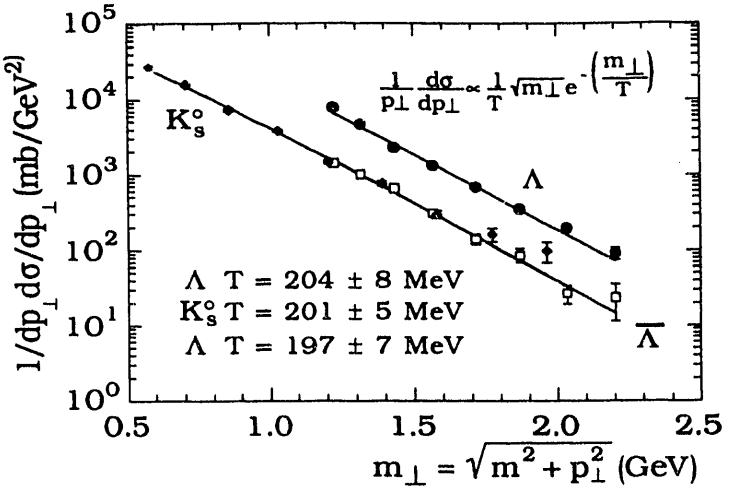

Fig.13 Transverse momentum distributions for Λ, $\bar{\Lambda}$ and K^o in S + Pb reactions.

6. Rapidity distributions

In p + p reactions, particles with a large sea quark content have a tendency to be produced at mid-rapidity as their partons are produced by string breaking. This simple reasoning gives some understanding of the tendency for $\bar{\Lambda}$ and K^o rapidity distributions to peak at mid rapidity while Λ peaks more toward the target or projectile regions due to its constituent quark content. Therefore rapidity distributions are a general indicator of the reaction mechanism. Below in Fig.14a we see the rapidity distributions measures by NA36 for Λ production in p + Pb reactions and S + Pb reactions. The distribution for p + Pb peaks towards target rapidity as expected, however, the distribution for S + Pb reactions peaks near mid-rapidity. This behavior clearly cannot be described as a simple superposition of p + N collisions as is shown in Fig.14b where the prediction of the model Fritiof 1.7 is compared with the data.

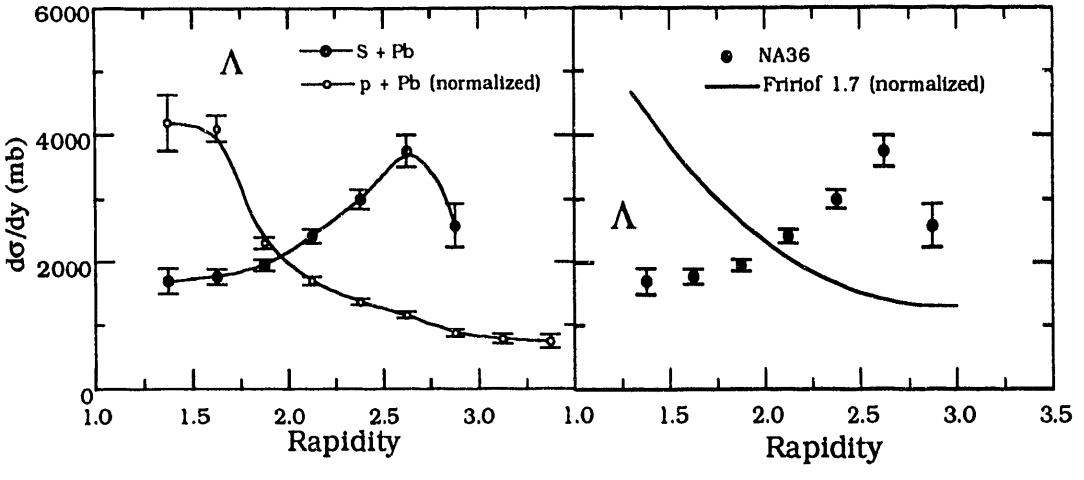

Fig.14a,b Λ rapidity distributions for p + Pb, S + Pb and Fritiof 1.7

Since such a unusual result may signify important changes in the reaction mechanism we now describe some of the extensive checks we have made of the correction procedures applied to the data.

The raw data is divided by acceptance and efficiency to produce the quoted cross sections. Acceptance was calculated to better than 5% accuracy in all cases by generating Monte Carlo V^0's and propagating them through the experimental apparatus and accepting them if they passed the cuts used on the data. Efficiency was calculated by embeding the accepted V^0's in actual events and running the analysis software to determine if they would be detected. In both the acceptance and efficiency calculations the origin of the V^0 was determined by actual empirical beam positions at the target taken from a set of representative data tapes. This positioning was done to properly account for the finite beam size. Efficiencies were calculated to an accuracy of 5-15%. The errors shown on all cross sections quoted include the contributions from the acceptance, efficiency and background subtraction. The efficiency for finding V^0's decreases with multiplicity reaching 5% at the highest multiplicities. To make sure that the distributions are not unduly affected by high multiplicity events we plot the multiplicity of events in which Λ's were found in Fig. 15. We conclude that the bulk of the observed signal comes from events at about 1/3-1/2 of the maximum multiplicity avoiding dominance of low efficiency data. Efficiency also changes with rapidity, this effect is shown in Fig. 16 where it is clear that we have our optimum detection efficiency in the region $1.7 < y < 2.5$ exactly where the rapidity distribution rises instead of dropping as the model predicts.

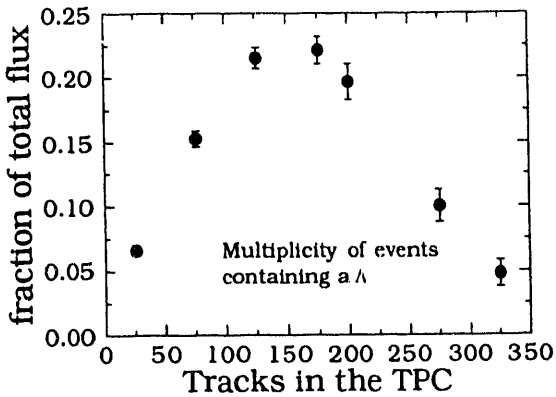

Fig. 15 Lambda event multiplicity

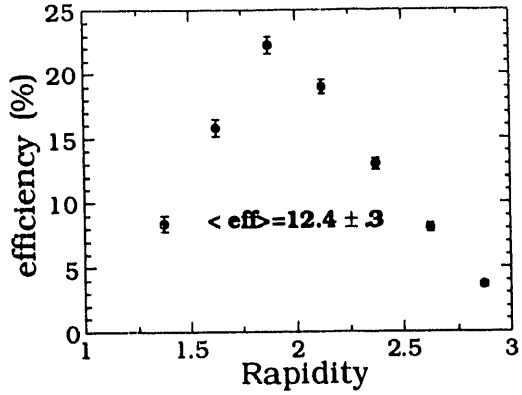

Fig.16 Efficiency vs rapidity

The acceptance and efficiency corrections will of course change the shape of the rapidity distribution. To see this change we have plotted the raw, acceptance corrected and efficiency corrected data in Fig.17. Here, the curves are normalized to the same area to allow comparison of their shapes. We see that the rise in cross section with rapidity is evident at all stages of the analysis. The effect is not introduced as a result of any of the corrections.

Another test of the correction methods was made possible by a data set with the M1 magnet set to the opposite (positive) polarity. The topology of lambda decays are not symmetric with respect to a field reversal because most of the momentum is carried by the proton. The proton track is stiff and the acceptance depends primarily on the trajectory of the soft pion. The positive polarity data favored bending the pion from lambda decays up into the TPC thus giving a 40% larger acceptance. Comparing the results of the two polarities therefore is a test of the entire signal extraction and correction methods. We did a low statistics extraction and correction of the positive polarity data and compare both data sets where there were sufficient statistics in Fig. 18. There is clear agreement between the two sets of data. The conclusion is that the correction process gives consistant answers when applied to data sets quite different in both acceptance and efficiency.

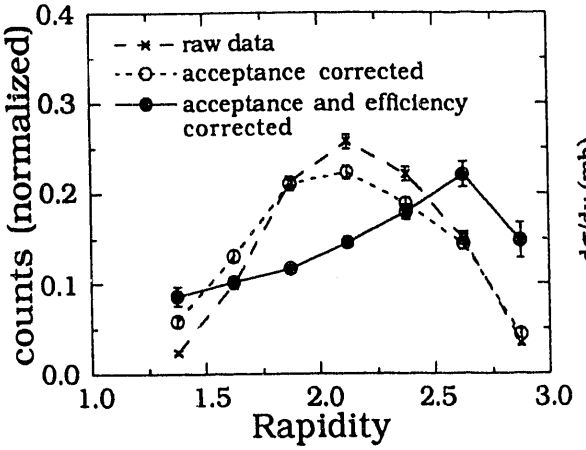

Fig.17 Raw and corrected Λ data.

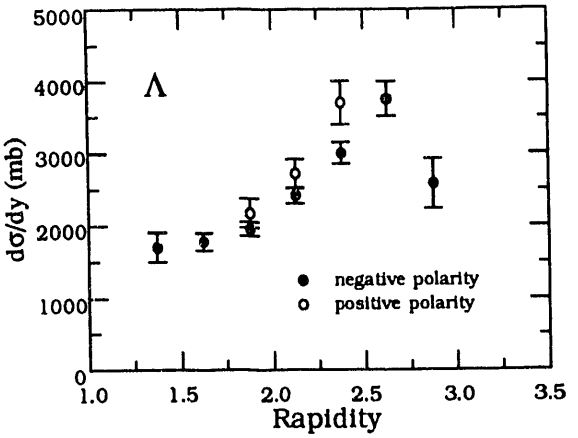

Fig. 18 Positive and negative polarity data.

The distributions for $\bar{\Lambda}$ and K^o are somewhat closer to what is seen in p + p data and are shown in Fig. 19a,b for p and S projectiles.

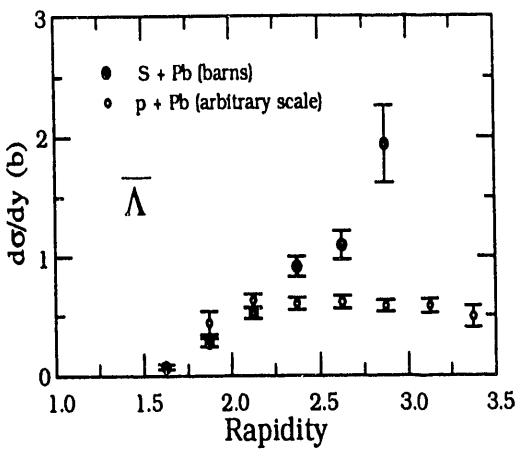

Fig.19a $\bar{\Lambda}$ rapidity distributions

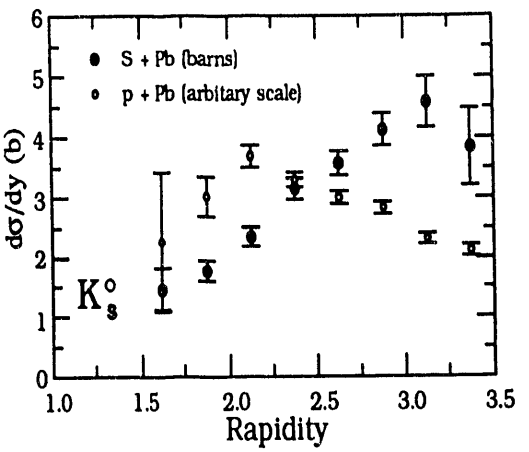

Fig. 19b K^o rapidity distributions.

If the mid-rapidity peak in the Λ cross section is due to a change in reaction mechanism when the number of participants increases it should also become weaker when the low multiplicity S + Pb reactions are examined. With the large statistics data of NA36 we are able to subdivide the Λ data into target rapidity region ($1.25 < y < 2.25$) and mid-rapidity region ($2.25 < y < 3.25$) the "cross section ratio" of production in these two regions then is a measure of the strength of the mid-rapidity peak. Fig.20 shows this ratio as a function of negative multiplicity and also the prediction from Fritiof 1.7. We see that the enhancement at mid-rapidity is a strong function of multiplicity and is not present at the lowest multiplicities. The Fritiof comparison shows that this dependence is not expected from superposition of nucleon - nucleon reactions.

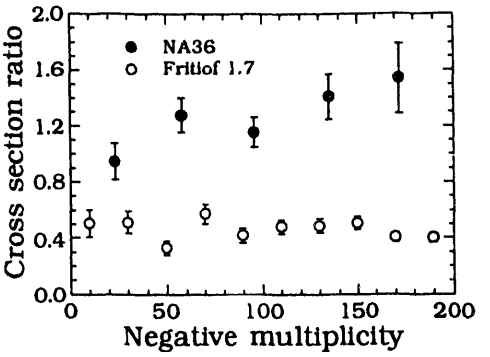

Fig. 20 Multiplicity dependence of the central rapidity peaking in Λ production.

7. Conclusions

The reactions of S + Pb at 200 GeV/c per nucleon have been found to have three interesting properties:

1. Strangeness is enhanced over p+ Pb reactions by roughly a factor of two.
2. Strange particle "temperatures" are near 200 MeV, which is the predicted region of quark-gluon plasma production.[6]
3. The rapidity distribution of Λ particles is increasingly peaked at mid-rapidity as the event multiplicity increases.

None of these properties are predicted by conventional models which use a superimposition of nucleon + nucleon reactions to simulate ion + ion reactions. We are thus lead to the conclusion that some other reaction mechanism is active. It should also be noted that these properties are qualitatively consistent with the production of a dense, deconfined fireball formed at mid-rapidity [7]. The experimental data in the ultra-relativistic ion-ion collisions has progressed to the point that it is imperative that quantitative predictions of non-superposition models be prepared and compared with existing data.

8. Acknowledgements

Part of this work was supported by EC grant A88000145; Director, Office of Energy Research, Division of Nuclear Physics of the Office of High Energy and Nuclear Physics of the U. S. Department of Energy under contract no. DE-AC03-76SF00098 and DE-FG02-91ER40652, United Kingdom Science and Engineering Research Council under Grant GR/F 40065 and Spain under CICYT contracts 85-0022, AE86-0031, AE87-0031, AE88-0031, AE89-0589, AE90-0031, AEN91-0739 and XUGA 80409288. The authors are grateful to CERN and IBM for support and use of the PPCS STAGE 2 computer system.

9. References

1. P. Koch, B.Müller and J. Rafelski, Physics Reports 142 (1986) 167.
2. NA36 Collaboration, Phys. Lett. B294 (1992) 127.
3. J. Bartke, et al., NA35 Collaboration, Z. für Phys., C48 (1990) 191.
4. S. Abatzis et al., WA85 Collaboration, Phys. Lett.,B244 (1990) 130.
5. CERN-TH. 4794/87 for comparison with energy flow see NA35 Collaboration, Z. Phys. C 52 (1991) 239.
6. A. Ukawa, Nucl. Phys. A498 (1989) 227c.
7. J. Rafelski, H. Rafelski and M. Danos, Phys.Lett. B294(1992)131.

END

DATE
FILMED
4/11/93